International Journal of Applied Engineering Research ISSN 0973-4562 Volume 13, Number 7 (2018) pp. 5501-5507

A New Application of Extreemum-Seeking Algorithm for PMSG-Wind turbine via Linear Quadratic Regulator

Dinh Chung, Phan and Thi Minh Dung, Tran

Faculty of Electrical Engineering, The University of Danang-University of Science and Technology, 550000, Danang, Vietnam.

Abstract

In this paper, a new application of extreemum-seeking (ES) algorithm for the maximum power output of a permanent magnetic synchronous generator (PMSG) wind turbine is proposed. A new control law for the machine side converter of PMSG is designed technically based on a cascade PI controller for both d-axis current and rotor speed adjustment to minimize the power loss in the stator winding of PMSG and to execute the extreemum-seeking purpose of the wind turbine respectively. Furthermore, the performance of this cascade PI controller is optimized by using Linear Quadratic Regulator (LQR). The proposed combination between a new control law and ES algorithm is evaluated by simulating a PMSG wind turbine in Matlab/Simulink. In which, the authors not only dug into the simulation results' analysis of a conventional method to express the effectiveness of the proposed one. The application of ES algorithm can be used instead of making use of exactly-known turbine knowledge since the wind turbine can track its maximum power point curve as well as the power loss in PMSG can reach the minimum.

Keywords: Extreemum seeking, Linear Quadratic Regulator, maximum power, PMSG-wind turbine, power loss.

INTRODUCTION

In literature, there are a lot of publications concerning to the maximum power point tracking of a wind turbine such as tip-speed ratio method, optimal torque method, power signal feedback, perturbation and observation method and so on [1], [2], [3], [4]. In which, the recent suggested methods make use of a neural network to estimate the wind speed [2], [3]. In execution, a sample datasheet must be normally required for training step [3] and obviously it is not easy to obtain this datasheet. Moreover, for a neural network application, the tip-speed ratio of wind turbine must be clarified "in priori" [2], [3]. Unfortunately, this parameter is pracitcally unknown. In [4] Extreemum-seeking (ES) algorithm was proposed to be used in wind turbine. However, this method has just applied to a squirrel-cage induction generator using in varying-speed wind turbine. Until now, the application of the ES algorithm to a PMSG wind turbine has not yet appeared in recent literature.

Concerning to control system, a PI controller is obviously well-known in wind turbine [5] because of its simplicity. However, the determination of PI controller parameters is not an easy task. In some cases, it cannot guarantee the stability and the adaptation of the PI controller parameters. To overcome this problem, a Linear Quadractic Regulator (LQR) was applied in PMSG-wind turbines [6] for DC voltage and current adjustment purpose. Another application of LQR in wind turbine is presented in [7]. In this research, LQR is used for PMSG wind turbine with a boost converter. However, the application of LQR for rotor speed adjustment in a PMSG wind turbine should be evaluated.

In this paper, we propose a new application of the ES algorithm to estimate the optimal tip-speed ratio and design a new control law for the machine side converter of a PMSG-wind turbine. The main purpose of this controller usage is to adjust both d-axis current and rotor speed such that the power loss in PMSG is the minimum while the power output of the wind turbine hits the maximum. This controller is designed based on cascade PI control and optimized by using Linear Quadratic Regulator. In Section 2, we first modelise the PMSG-wind turbine system and express our statement. Next, the objectives of a MSC controller are determined in Section 3 before executing its design in Section 4. By using Matlab/Simulink, the performance of the proposed scheme is evaluated. And, to prove for the efficiency, a comparison of this scheme to the case of a conventional method is then carried out in section 5.

MODELIZATION OF A PMSG_WIND TURBINE

Theoretically, a PMSG wind turbine structure is to connect a wind turbineto a permanent magnetic synchronous generator (PMSG) through a shaft and gearbox system as shown in Figure 1a. To interface with a grid, a full AC-DC-AC power converter, including a machine-side converter (MSC), a grid-side converter (GSC), and a DC-link, is installed in the stator side, in [5].

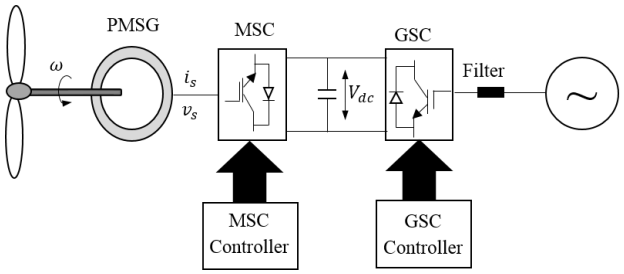

(a)

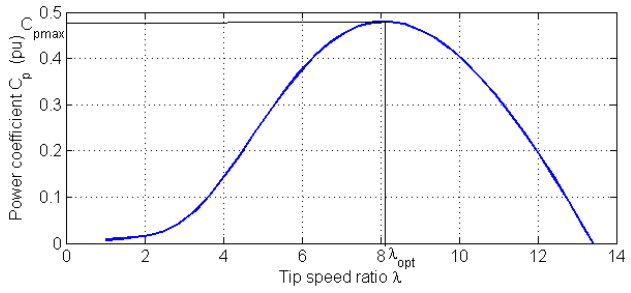

(b)

Figure 1. Overall system of a PMSG wind turbine: (a) the structure of PMSG wind turbine and (b) an example of the wind turbine's power coefficient.

Wind turbine

The main duty of a wind turbine is to convert wind's kinetic energy to mechanical energy on the turbine shaft. Mechanical power on the turbine shaft at wind speed V_w and its rotor speed ω is computed as follows, in [5]:

$$P_m(t) = \frac{1}{2}\rho\pi R^2 C_p(\lambda,\beta)V_w^3(t), \quad (1)$$

where ρ and R are air density and wind's turbine blade length, while $C_p(\lambda,\beta)$ is the power coefficient which indicates the percentage of the wind kinetic power converted to the mechanical power with λ, β being the tip-speed ratio and the pitch angle respectively. In [5], the turbine's power coefficient depends on both tip speed ratio λ and pitch angle β which is defined as follows:

$$\lambda(t) = \frac{R\omega(t)}{V_w(t)} \quad (2)$$

However, in this paper, the authors only consider the maximum power extraction of the wind turbine. Taking Figure 1b as an example, at a constant pitch angle β, the power coefficient $C_p(\lambda,\beta)$ has a maximum point at λ_{opt}. Here, the maximum power coefficient can be defined as follows:

$$C_{pmax} = \max_{\lambda} C_p(\lambda,0) = C_p(\lambda_{opt},0) \quad (3)$$

Therefore, for this purpose, we assume that the pitch angle is kept at zero, $\beta = 0$.

As a result, when the wind turbine operates at $\lambda = \lambda_{opt}$ then the mechanical power of the wind turbine becomes maximum:

$$P_{max}(t) = \frac{1}{2}\rho\pi R^2 C_{pmax}V_w^3(t), \quad (4)$$

And the mechanical torque of wind turbine, in [5] is defined as follows:

$$T_m(t) = \frac{P_m(t)}{\omega(t)} \quad (5)$$

PMSG

PMSG is to convert the mechanical power on its shaft to the electrical one on its stator winding. The motion equation of PMSG-wind turbine is:

$$J\frac{d}{dt}\omega(t) = -f\omega(t) + T_m(t) - T_e(t) \quad (6)$$

where $T_m$is mechanical torque, T_e is the electrical torque, while f is the damping coefficient of the PMSG-wind turbine system.

In dq frame, the electrical circuit of a nonsilent rotor PMSG [5] is described as Figure 2, where v are the voltage and current of the stator winding; $\psi_f$is rotor flux; $R_s$is the stator winding resistance; L is the inductance of stator winding; subscripts d and q stand for the d and q axis. From Figure 2, we have:

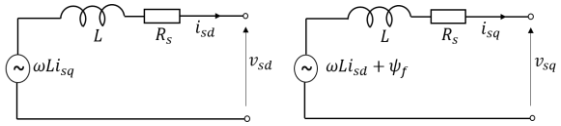

(a) **(b)**

Figure 2. Equivalent circuit of a PMSG wind turbine in dq frame: (a) d axis and (b) q axis.

$$L\frac{d}{dt}\boldsymbol{i_s}(t) = -R_s\boldsymbol{i_s}(t) + \boldsymbol{v_s}(t) - L\boldsymbol{\Theta}\boldsymbol{i_s}(t)\omega(t) - [0 \quad 1]^T\omega(t)\psi_f \quad (7)$$

$$\boldsymbol{v_s} = [v_{sd} \quad v_{sq}]^T;\ \boldsymbol{i_s} = [i_{sd} \quad i_{sq}]^T;\ \boldsymbol{\Theta} = \begin{bmatrix}0 & -1\\ 1 & 0\end{bmatrix}.$$

In [5], the electromagnetic torque is defined:

$$T_e(t) = \frac{3}{2}n_p\psi_f i_{sq}(t) = K_T i_{sq}(t), \quad (8)$$

where $n_p$is the number of pole pairs.

Power loss in the stator winding of PMSG is:

$$\Delta P_{loss} = R_s i_s^2 = R_s\left(i_{sd}^2 + i_{sq}^2\right), \quad (9)$$

From (6), (7), and (8), the PMSG wind turbine is described as follows:

$$\begin{cases}\frac{d}{dt}\boldsymbol{x}(t) = \boldsymbol{A}\boldsymbol{x}(t) + \frac{1}{L}\boldsymbol{B}\boldsymbol{v_s}(t) + \boldsymbol{E}d(t) - \begin{bmatrix}0\\ \boldsymbol{\Theta}\end{bmatrix}\omega(t)\boldsymbol{i_s}(t)\\ \boldsymbol{y}(t) = \boldsymbol{C}\boldsymbol{x}(t) + \boldsymbol{F}d(t)\end{cases} \quad (10)$$

where $\boldsymbol{v_s}$ is control variable, $\boldsymbol{y}$ is the output of the system,

$$\boldsymbol{x} = [\omega \quad i_{sd} \quad i_{sq}]^T,\ d = T_m, \quad (11)$$

$$\boldsymbol{A} = \begin{bmatrix}-\frac{f}{J} & 0 & -\frac{K_T}{J}\\ 0 & -\frac{R_s}{L} & 0\\ -\frac{\psi_f}{L} & 0 & -\frac{R_s}{L}\end{bmatrix} \in R^{3\times3},$$

$$\boldsymbol{B} = \begin{bmatrix}\boldsymbol{0}\\ \boldsymbol{I}_2\end{bmatrix}^T \in R^{3\times2},\ \boldsymbol{C} = \begin{bmatrix}\boldsymbol{I}_3\\ \boldsymbol{0}\end{bmatrix} \in R^{4\times3},$$

$$\boldsymbol{E} = \frac{1}{J}\begin{bmatrix}1\\ \boldsymbol{0}_{2\times1}\end{bmatrix},\ \boldsymbol{F} = \begin{bmatrix}\boldsymbol{0}_{3\times1}\\ 1\end{bmatrix}. \quad (12)$$

CONTROL OBJECTIVES FOR MSC

In this paper, the authors aim to force the wind turbine to be able to track the maximum power point as well as to make the power loss in the stator winding of PMSG reach the minimum.

Maximum power point tracking

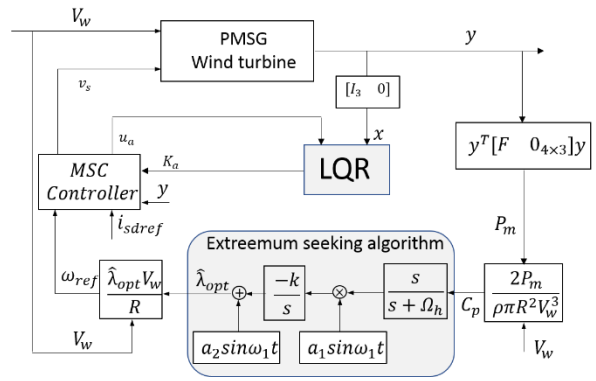

(a)

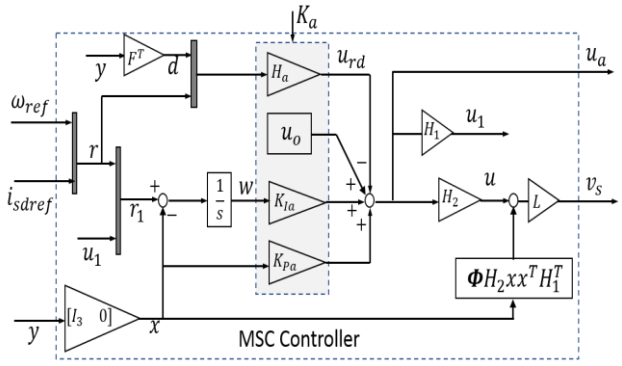

(b)

Figure 3. Proposal MPPT method for PMSG wind turbine: (a) New application of extreemum seeking and (b) MSC controller.

To track maximum power point, the wind turbine velocity ω must be maintained at ω_{opt}:

$$\omega_{opt}(t) = \frac{\lambda_{opt} V_w(t)}{R} \tag{13}$$

Practically $\lambda_{opt}$is unknown. Therefore, to obtain ω_{opt}, in this paper, we embed the ES algorithm, in [9], to estimate the optimal tip speed ratio, $\hat{\lambda}_{opt}$. As mentioned in subsection 2.1, as $\beta = 0$, $C_p(\lambda)$ has a unique maximum point at λ_{opt}. Hence, to successfully apply the ES algorithm, $C_p(\lambda)$ must be computed online from (1) as follows:

$$C_p(\lambda) = \frac{2P_m(t)}{\rho \pi R^2 V_w^3(t)}, \tag{14}$$

In Figure 3a the ES algorithm is embedded in the PMSG wind turbine, where

$$P_m = \omega T_m = \omega d = \boldsymbol{y}^T [\boldsymbol{F} \quad \boldsymbol{0}_{4\times 3}] \boldsymbol{y} \tag{15}$$

In this figure, $\Omega_h, \omega_1, k, a_1$are designed parameters. And

$$\hat{\lambda}_{opt} = \lambda_{opt} + \epsilon, \tag{16}$$

where ϵ is the ES algorithm's error which proof has been proposed in [8]. Hence, we can estimate the optimal rotor speed as:

$$\widehat{\omega}_{opt} = \frac{\hat{\lambda}_{opt} V_w}{R} \tag{17}$$

Minimum power loss

To minimize the power loss, $i_{sd} = 0$ should be remained, in (9). As a result, the power loss in the stator winding of PMSG is only affected by i_{sq} which depends on the active power output of PMSG.

In conclusion, to obtain maximum power point tracking and minimize power loss simultaneously, the MSC controller is to be designed subject to:

$$\omega \to \omega_{ref} = \widehat{\omega}_{opt}, i_{sd} \to i_{sdref} = 0. \tag{18}$$

MSC CONTROLLER DESIGN

In this paper, we only propose a new control law for MSC as shown in Figure 3b. Here, the output from the controller is v_s, defined as follows:

$$\boldsymbol{v_s}(t) = L\boldsymbol{u}(t) + \omega(t)\boldsymbol{\Theta i_s}(t), \tag{19}$$

where $\boldsymbol{u} = [u_d \quad u_q]^T$ is a new control signal to be designed. The dynamics of the system (10) is

$$\begin{cases} \frac{d}{dt}x(t) = \boldsymbol{A}\boldsymbol{x}(t) + \boldsymbol{B}\boldsymbol{u}(t) + \boldsymbol{E}d(t) \\ \boldsymbol{y}(t) = \boldsymbol{C}\boldsymbol{x}(t) + \boldsymbol{F}d(t) \end{cases}. \tag{20}$$

The purpose of this controller is to minimize the error, defined as follows:

$$\boldsymbol{e}(t) = \boldsymbol{r}_1(t) - \boldsymbol{x}(t) \in R^3, \tag{21}$$

where

$$\boldsymbol{r}_1(t) = [\boldsymbol{r}(t) \quad u_1(t)]^T, \ \boldsymbol{r} = [\omega_{ref} \quad i_{sdref}]^T. \tag{22}$$

Here, u_1 is the reference value of i_{sq}.

Let $\boldsymbol{w}(t) = \int_0^t \boldsymbol{e}(\tau)d\tau$, where $\boldsymbol{w}(t) = [w_1 \quad w_2 \quad w_3]^T$. It means that

$$\frac{d}{dt}\boldsymbol{w}(t) = \boldsymbol{r}_1(t) - \boldsymbol{x}(t). \tag{23}$$

By using (22), we can rewrite (23) as:

$$\frac{d}{dt}\boldsymbol{w}(t) = -\boldsymbol{I}_3\boldsymbol{x}(t) + \boldsymbol{D}\boldsymbol{r}(t) + \boldsymbol{B}_1\boldsymbol{u}_1(t) \tag{24}$$

where $= [\boldsymbol{I}_2 \quad \boldsymbol{0}]^T \in R^{3\times 2}$, $\boldsymbol{B}_1 = [0 \quad 0 \quad 1]^T \in R^{3\times 1}$.

To adjust the rotor speed, we must adjust i_{sq} according to (6) and (8). Hence, u_1 is a virtual control input. From (20) and (24), the augmented system is

$$\frac{d}{dt}\boldsymbol{x}_a(t) = \boldsymbol{A}_a\boldsymbol{x}_a(t) + \boldsymbol{B}_a\boldsymbol{u}_a(t) + \boldsymbol{G}_a\begin{bmatrix} d(t) \\ \boldsymbol{r}(t) \end{bmatrix}, \tag{25}$$

where

$$\boldsymbol{x}_a = \begin{bmatrix} \boldsymbol{x} \\ \boldsymbol{w} \end{bmatrix} \in R^{6\times 1}, \boldsymbol{u}_a = \begin{bmatrix} u_1 \\ \boldsymbol{u} \end{bmatrix} \in R^{3\times 1}, \tag{26}$$

$$\boldsymbol{A}_a = \begin{bmatrix} \boldsymbol{A} & \boldsymbol{0} \\ -\boldsymbol{I}_3 & \boldsymbol{0} \end{bmatrix} \in R^{6\times 6},$$

$$\boldsymbol{B}_a = \begin{bmatrix} \boldsymbol{0} & \boldsymbol{B} \\ \boldsymbol{B}_1 & \boldsymbol{0} \end{bmatrix} \in R^{3\times 6},$$

$$\boldsymbol{G}_a = \boldsymbol{E} \oplus \boldsymbol{D} \in R^{6\times 3}. \quad (27)$$

In the steady state, (25) satisfies

$$\begin{bmatrix} \boldsymbol{A} & \boldsymbol{0} \\ -\boldsymbol{I}_3 & \boldsymbol{0} \end{bmatrix} \begin{bmatrix} \boldsymbol{x}_\infty \\ \boldsymbol{w}_\infty \end{bmatrix} + \begin{bmatrix} \boldsymbol{0} & \boldsymbol{B} \\ \boldsymbol{B}_1 & \boldsymbol{0} \end{bmatrix} \boldsymbol{u}_{a\infty} + \boldsymbol{G}_a \begin{bmatrix} d_\infty \\ \boldsymbol{r}_\infty \end{bmatrix} = 0 \quad (28)$$

Hence,

$$\boldsymbol{G}_a \begin{bmatrix} d_\infty \\ \boldsymbol{r}_\infty \end{bmatrix} = \begin{bmatrix} \boldsymbol{A} & \boldsymbol{0} & \boldsymbol{B} \\ -\boldsymbol{I}_3 & \boldsymbol{B}_1 & \boldsymbol{0} \end{bmatrix} \begin{bmatrix} \boldsymbol{x}_\infty \\ \boldsymbol{u}_{a\infty} \end{bmatrix}. \quad (29)$$

The system error is

$$\frac{d}{dt}\tilde{\boldsymbol{x}}_a(t) = \boldsymbol{A}_a\tilde{\boldsymbol{x}}_a(t) + \boldsymbol{B}_a\tilde{\boldsymbol{u}}_a(t) + \boldsymbol{G}_a\tilde{\boldsymbol{\xi}}(t), \quad (30)$$

where $\tilde{\boldsymbol{x}}_a = \boldsymbol{x}_a - \boldsymbol{x}_{a\infty}, \tilde{\boldsymbol{u}}_a = \boldsymbol{u}_a - \boldsymbol{u}_{a\infty}, \tilde{\boldsymbol{\xi}} = \begin{bmatrix} d - d_\infty \\ \boldsymbol{r} - \boldsymbol{r}_\infty \end{bmatrix}$. In (30), we supposed $\tilde{\boldsymbol{\xi}}$ is a white noise. Then, the system error must be stabilized by

$$\tilde{\boldsymbol{u}}_a = \boldsymbol{K}_a\tilde{\boldsymbol{x}}_a \quad (31)$$

where $\boldsymbol{K}_a \in R^{3\times 6}$ is a feedback gain. To determine $\boldsymbol{K}_a$, Linear Quadratic Regular is used to minimize

$$J_a = \int_0^\infty (\tilde{\boldsymbol{x}}_a{}^T\boldsymbol{Q}_a\tilde{\boldsymbol{x}}_a + \tilde{\boldsymbol{u}}_a{}^T\boldsymbol{R}_a\tilde{\boldsymbol{u}}_a)d\tau, \quad (32)$$

where $\boldsymbol{Q}_a \geq 0, \boldsymbol{Q}_a \in R^{6\times 6}$ and $\boldsymbol{R}_a \geq 0, \boldsymbol{R}_a \in R^{3\times 3}$. An optimal control signal input is given as:

$$\tilde{\boldsymbol{u}}_a = -\boldsymbol{R}_a{}^{-1}\boldsymbol{B}_a{}^T\boldsymbol{P}_a\tilde{\boldsymbol{x}}_a, \quad (33)$$

where $\boldsymbol{P}_a$ is a semi-definite symmetric matrix ($\boldsymbol{P}_a \geq 0$, $\boldsymbol{P}_a \in R^{3\times 3}$) and satisfies the Riccati equation [9]

$$\boldsymbol{A}_a{}^T\boldsymbol{P}_a + \boldsymbol{P}_a\boldsymbol{A}_a - \boldsymbol{P}_a\boldsymbol{B}_a\boldsymbol{R}_a{}^{-1}\boldsymbol{B}_a{}^T\boldsymbol{P}_a + \boldsymbol{Q}_a = 0. \quad (34)$$

Hence, the optimal feedback gain is given by

$$\boldsymbol{K}_a = -\boldsymbol{R}_a{}^{-1}\boldsymbol{B}_a{}^T\boldsymbol{P}_a = -\boldsymbol{R}_a{}^{-1}\boldsymbol{B}_a{}^T\begin{bmatrix} \boldsymbol{P}_{11} & \boldsymbol{P}_{12} \\ \boldsymbol{P}_{21} & \boldsymbol{P}_{22} \end{bmatrix} \quad (35)$$

and the optimal control signal input $u_a$is

$$\begin{aligned} \boldsymbol{u}_a &= \boldsymbol{K}_a\begin{bmatrix} \boldsymbol{x} \\ \boldsymbol{w} \end{bmatrix} - \boldsymbol{K}_a\begin{bmatrix} \boldsymbol{x}_\infty \\ \boldsymbol{w}_\infty \end{bmatrix} + \boldsymbol{u}_{a\infty} \\ &= \boldsymbol{K}_{Pa}\boldsymbol{x} + \boldsymbol{K}_{Ia}\boldsymbol{w} + \boldsymbol{u}_{a\infty} - \boldsymbol{K}_{Pa}\boldsymbol{x}_\infty - \boldsymbol{K}_{Ia}\boldsymbol{w}_\infty \quad (36) \end{aligned}$$

where

$$\boldsymbol{P}_a = \begin{bmatrix} \boldsymbol{P}_{11} & \boldsymbol{P}_{12} \\ \boldsymbol{P}_{21} & \boldsymbol{P}_{22} \end{bmatrix} \in R^{6\times 6},$$

$$\boldsymbol{K}_{Pa} = -\boldsymbol{R}_a{}^{-1}\begin{bmatrix} \boldsymbol{B}_1{}^T\boldsymbol{P}_{21} \\ \boldsymbol{B}^T\boldsymbol{P}_{11} \end{bmatrix} \in R^{3\times 3},$$

$$\boldsymbol{K}_{Ia} = -\boldsymbol{R}_a{}^{-1}\begin{bmatrix} \boldsymbol{B}_1{}^T\boldsymbol{P}_{22} \\ \boldsymbol{B}^T\boldsymbol{P}_{12} \end{bmatrix} \in R^{3\times 3}. \quad (37)$$

When the steady state of the integrator $w_\infty$is set as

$$\boldsymbol{w}_\infty = \boldsymbol{w}(0) - \boldsymbol{P}_{22}{}^{-1}\boldsymbol{P}_{12}{}^T(\boldsymbol{x}(0) - \boldsymbol{x}_\infty), \quad (38)$$

we can obtain the cost function:

$$\min_{w(0)}\min_{\tilde{u}_a} J_a = \boldsymbol{x}(0)^T(\boldsymbol{P}_{11} - \boldsymbol{P}_{12}\boldsymbol{P}_{22}{}^{-1}\boldsymbol{P}_{12}{}^T)\boldsymbol{x}(0) \quad (39)$$

From (36) and (38), we have

$$\begin{aligned} \boldsymbol{u}_a &= \boldsymbol{K}_{Pa}\boldsymbol{x} + \boldsymbol{K}_{Ia}\boldsymbol{w} + \boldsymbol{u}_{a\infty} - \boldsymbol{K}_{Pa}\boldsymbol{x}_\infty - \boldsymbol{K}_{Ia}\boldsymbol{w}(0) \\ &\quad - \boldsymbol{K}_{Ia}\boldsymbol{P}_{22}{}^{-1}\boldsymbol{P}_{12}{}^T(\boldsymbol{x}(0) - \boldsymbol{x}_\infty), \\ &= \boldsymbol{K}_{Pa}\boldsymbol{x} + \boldsymbol{K}_{Ia}\boldsymbol{w} - \boldsymbol{K}_{Ia}\boldsymbol{w}(0) - \boldsymbol{K}_{Ia}\boldsymbol{P}_{22}{}^{-1}\boldsymbol{P}_{12}{}^T\boldsymbol{x}(0) \\ &\quad + \boldsymbol{u}_{a\infty} - \boldsymbol{K}_{Pa}\boldsymbol{x}_\infty + \boldsymbol{K}_{Ia}\boldsymbol{P}_{22}{}^{-1}\boldsymbol{P}_{12}{}^T\boldsymbol{x}_\infty \\ &= \boldsymbol{K}_{Pa}\boldsymbol{x} + \boldsymbol{K}_{Ia}\boldsymbol{w} - \boldsymbol{K}_{Ia}\boldsymbol{w}(0) - \boldsymbol{K}_{Ia}P_{22}{}^{-1}\boldsymbol{P}_{12}{}^T\boldsymbol{x}(0) \\ &\quad + [-\boldsymbol{K}_{Pa} + \boldsymbol{K}_{Ia}\boldsymbol{P}_{22}{}^{-1}\boldsymbol{P}_{12}{}^T \quad \boldsymbol{I}_3]\begin{bmatrix} \boldsymbol{x}_\infty \\ \boldsymbol{u}_{a\infty} \end{bmatrix}, \quad (40) \end{aligned}$$

By substituting (28) into (40), we have

$$\begin{aligned} \boldsymbol{u}_a &= \boldsymbol{K}_{Pa}\boldsymbol{x} + \boldsymbol{K}_{Ia}\boldsymbol{w} - \boldsymbol{K}_{Ia}\boldsymbol{w}(0) - \boldsymbol{K}_{Ia}\boldsymbol{P}_{22}{}^{-1}\boldsymbol{P}_{12}{}^T\boldsymbol{x}(0) \\ &+ [-\boldsymbol{K}_{Pa} + \boldsymbol{K}_{Ia}\boldsymbol{P}_{22}{}^{-1}\boldsymbol{P}_{12}{}^T \quad \boldsymbol{I}_3]\begin{bmatrix} \boldsymbol{A} & \boldsymbol{0} & \boldsymbol{B} \\ -\boldsymbol{I}_3 & \boldsymbol{B}_1 & \boldsymbol{0} \end{bmatrix}^{-1}\boldsymbol{G}_a\begin{bmatrix} d_\infty \\ \boldsymbol{r}_\infty \end{bmatrix} \\ &= \boldsymbol{K}_{Pa}\boldsymbol{x} + \boldsymbol{K}_{Ia}\boldsymbol{w} + \boldsymbol{u}_0 - \boldsymbol{u}_{rd} \quad (41) \end{aligned}$$

where

$$\boldsymbol{u}_0 = -\boldsymbol{K}_{Ia}\boldsymbol{w}(0) + \boldsymbol{H}_0\boldsymbol{x}(0), \ \boldsymbol{u}_0 = \boldsymbol{H}_a\begin{bmatrix} d_\infty \\ r_\infty \end{bmatrix}, \quad (42)$$

$$\boldsymbol{H}_0 = -\boldsymbol{K}_{\mathrm{Ia}}\,\boldsymbol{P}_{22}{}^{-1}\boldsymbol{P}_{12}{}^T \quad (43)$$

$$\boldsymbol{H}_a = [-\boldsymbol{K}_{Pa} + \boldsymbol{K}_{Ia}\boldsymbol{P}_{22}{}^{-1}\boldsymbol{P}_{12}{}^T \quad \boldsymbol{I}_3]\begin{bmatrix} \boldsymbol{A} & \boldsymbol{0} & \boldsymbol{B} \\ -\boldsymbol{I}_3 & \boldsymbol{B}_1 & \boldsymbol{0} \end{bmatrix}^{-1}\boldsymbol{G}_a$$

In summary, the control signal is

$$\boldsymbol{u}_1 = \boldsymbol{H}_1\boldsymbol{u}_{a,}, \boldsymbol{u} = \boldsymbol{H}_2\boldsymbol{u}_{a,} \quad (44)$$

$$\boldsymbol{H}_1 = \begin{bmatrix} 1 \\ 0 \\ 0 \end{bmatrix}, \boldsymbol{H}_2 = \begin{bmatrix} 0 & 0 \\ 1 & 0 \\ 0 & 1 \end{bmatrix}.$$

Hence,

$$\boldsymbol{v}_s = L(\boldsymbol{H}_2\boldsymbol{u}_a + \omega\boldsymbol{\Theta}\boldsymbol{i}_s) = L(\boldsymbol{H}_2\boldsymbol{u}_a + \boldsymbol{\Theta}\boldsymbol{H}_2\boldsymbol{x}\boldsymbol{x}^T\boldsymbol{H}_1{}^T) \quad (45)$$

where we used $\omega = \boldsymbol{x}^T\boldsymbol{H}_1{}^T$, $\boldsymbol{i}_s = \boldsymbol{H}_2\boldsymbol{x}$.

SIMULATION RESULT

In this section, we simulate a PMSG wind turbine using the proposed control law (45) and the embedded extremum-seeking method via Matlab/simulink. Here, we use a PMSG wind turbine with parameters as shown in Table1, in [10, 11], and its power coefficient is

$$C_p(\lambda,\beta) = 0.5176\left(\frac{116}{\lambda_i} - 0.4\beta - 5\right)e^{\frac{-21}{\lambda_i}} + 0.0068\lambda$$

$$\frac{1}{\lambda_i} = \frac{1}{\lambda+0.08\beta} - \frac{0.035}{\beta^3+1}, \quad (46)$$

and it has C_p curve versus λ as Figure 1b.

Table 1. Parameter of PMSG-wind turbine

Name	Value	
	SI unit	pu unit
Rated power P_{rated}	20MW	1
Rated rotor speed ω_{rated}	22.5rpm	1
Winding inductance L	1.5731mH	0.4538
Inertia of system J	6.5x106kgm^2	4.5s
Blade length R	40m	1
Rated voltage V_{srated}	690V	1
Winding resistance R_s	0.821mΩ	0.00387
Rated rotor flux ψ_f	5.826Wb	0.896
Damping coeficient f	35x103$\frac{Nms}{rad}$	0.1

From this figure, $C_p$has a maximum point at $\lambda_{opt} = 8.123$ $C_{pmax} = 0.48,$ as $\beta = 0$.

From the parameters in Table1, we have

$$\boldsymbol{A} = \begin{bmatrix} -0.02 & 0 & -0.02 \\ 0 & -0.01 & 0 \\ -1.97 & 0 & -0.1 \end{bmatrix},$$

$$\boldsymbol{B} = \begin{bmatrix} 0 & 0 \\ 2.2 & 0 \\ 0 & 2.2 \end{bmatrix}, \boldsymbol{E} = \begin{bmatrix} 0.22 \\ 0 \\ 0 \end{bmatrix}$$

Hence,

$\boldsymbol{Q} = \boldsymbol{Q}_1 \oplus \boldsymbol{Q}_2$, $\boldsymbol{R} = 10^{-2}\boldsymbol{I}_3$, $\boldsymbol{Q}_1 = 10^{-2}(4 \oplus \boldsymbol{I}_2)$, $\boldsymbol{Q}_2 = 10^3\boldsymbol{I}_3$.

Hence, we can calculate

$$\boldsymbol{P}_{11} = \begin{bmatrix} 23.83 & 0 & -0.56 \\ 0.00 & 0.007 & 0 \\ -0.56 & 0 & 0.02 \end{bmatrix},$$

$$\boldsymbol{P}_{12} = \begin{bmatrix} -78.45 & 0 & -0.01 \\ 0 & -1.43 & 0 \\ 1.43 & 0 & -0.01 \end{bmatrix},$$

$$\boldsymbol{P}_{21} = \begin{bmatrix} -78.45 & 0 & 1.43 \\ 0 & -1.43 & 0 \\ 0 & 0 & -0.01 \end{bmatrix},$$

$$\boldsymbol{P}_{22} = \begin{bmatrix} 396.57 & 0 & 0.02 \\ 0 & 53.66 & 0 \\ 0.02 & 0 & 3.16 \end{bmatrix},$$

and then, we can obtain

$$\boldsymbol{K}_{Pa} = \begin{bmatrix} -2.13 & 0 & -316.23 \\ 0 & 316.23 & 0 \\ -316.23 & 0 & 2.13 \end{bmatrix},$$

$$\boldsymbol{K}_{Ia} = \begin{bmatrix} 0.85 & 0 & 0.97 \\ 0.00 & -16.96 & 0 \\ 123.96 & 0 & -4.94 \end{bmatrix},$$

$$\boldsymbol{H}_a = \begin{bmatrix} 1.12 & -0.11 & 0 \\ 0 & 0 & 8.51 \\ 4.23 & -62.72 & 0 \end{bmatrix},$$

$$\boldsymbol{H}_0 = \begin{bmatrix} 0.85 & 0 & 0.97 \\ 0 & -8.46 & 0 \\ 62.82 & 0 & -1.15 \end{bmatrix}.$$

Here, we set $\boldsymbol{x}(0) = [0.6 \quad 0 \quad 0]^T$and $\boldsymbol{w}(0) = [0 \quad 0 \quad 0]^T$.

Verification of the proposed control law

To verify the proposed control law in Figure 3b and compare its performance to a conventional cascade PI controller [5], we suppose that the tip-speed ratio λ_{opt} is know exactly, and so the referent rotor speed $\omega_{ref} = \omega_{opt}$is calculated as (13). Here, we simulate the PMSG-wind turbine with two wind-speed conditions, which are constant and variable speed.

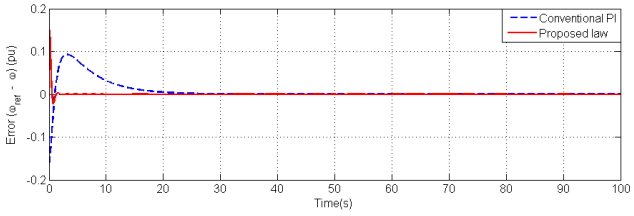

(a)

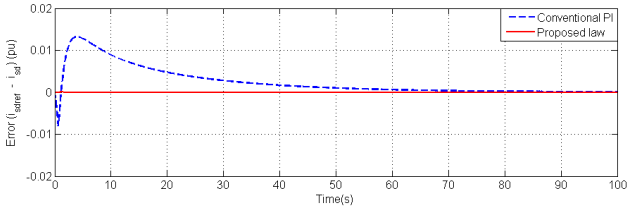

(b)

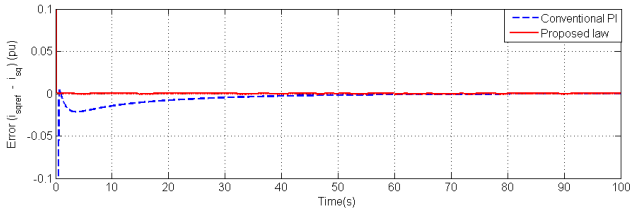

(c)

Figure 4. Simulation results for the proposed control law at a constant wind speed 10m/s: (a) error in rotor speed, (b) error in d-axis current, and (c) error in q-axis current.

When the wind speed is kept at constant 10m/s, the simulation result is shown in Figure 4. As can be seen from this figure, the errors in rotor speed, d and q-axis current

tent to zero. Therefore, the rotor speed ω and the d-axis currenti_{sd} approach to the reference $\omega_{ref} = \omega_{opt}$ and i_{sdref}. In other words, the objectives of the proposed control law are satisfied. Comparing to the result by using the conventional PI controller, it is easy to see that by using the proposed law, the errors approach to zero faster. This depicts that the proposed controller is better than the conventional PI one.

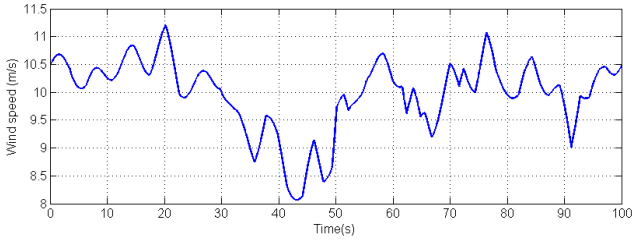

(a)

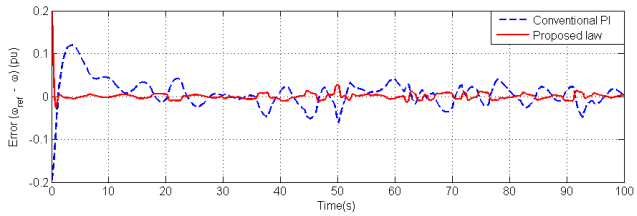

(b)

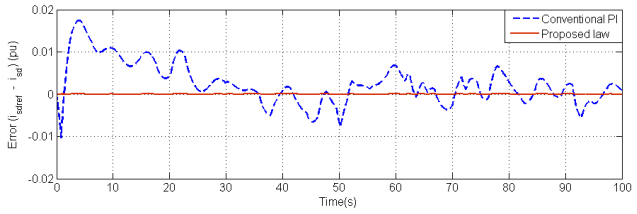

(c)

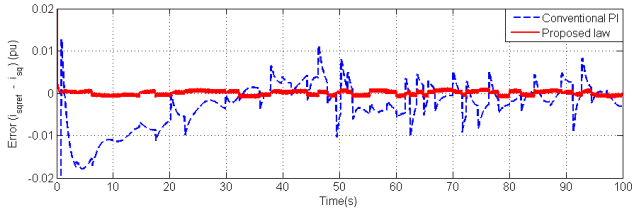

(d)

Figure 5. Simulation results for the proposed control law at a variable wind speed: (a) wind speed, (b) error in rotor speed, (c) error in d-axis current, and (d) error in q-axis current.

When the wind speed varies as Figure 5a, the simulation result is shown in Figure 5b to 5d. Clearly, by using the proposed control law, the error between reference and actual value is smaller than that by using the conventional PI. It means that the performance of the proposed controller gives more effective.

Verification of the new ES algorithm application

In this subsection, we verify the PMSG-wind turbine with the embedded ES application and the proposed control law. Firstly, as can be seen in Figure 3, the reference of the rotor speed is determined by $\hat{\lambda}_{opt}$ which is the output of the ES algorithm. In Figure 5a, with data of the wind velocity, the simulation result shown in Figure 6, where the red curve represents for $\hat{\lambda}_{opt}$ estimated by the new ES application and the dash blue curve is dedicated for λ_{opt} assumes that λ_{opt} is known.

From Figure 6a, the errors of the rotor speed for both cases are not similar. This error involves the perturbation signal $a_2 sin\omega_1 t$ used in the ES algorithm. However, for the d-axis current, the errors in two cases are similar, as described in Figure 6b. The tip-speed ratio λ is almost remained at the optimal value λ_{opt}as the case of known λ_{opt}, excepted from the beginning period, during which the ES algorithm is searching maximum point. Analogically, C_P reaches to its maximum value after this beginning period. On the other hand, the power losses in the stator winding in two cases are also similar as illustrated in Figure 6d. Obviously, the new ES application has performance like the case of known λ_{opt}, apart from the beginning period. Therefore, the new ES application can be definitely applied in the case of unknown λ_{opt}.

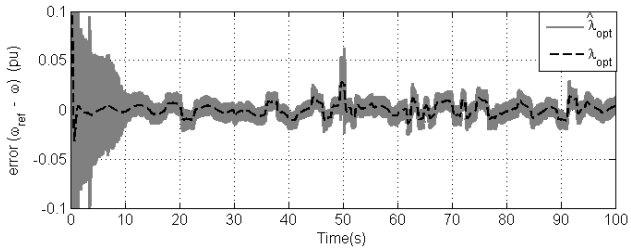

(a)

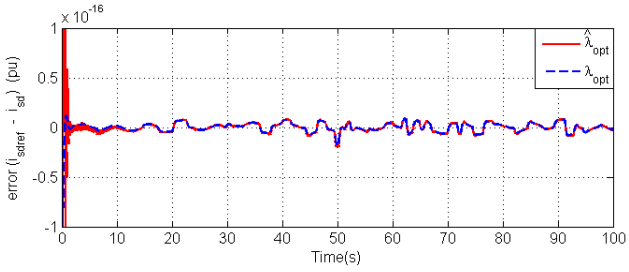

(b)

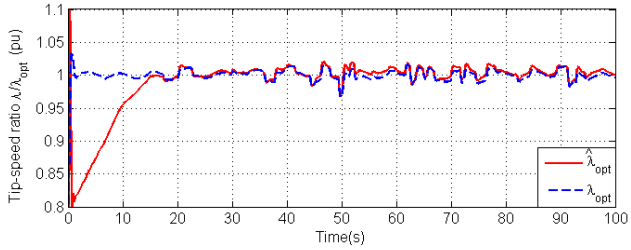

(c)

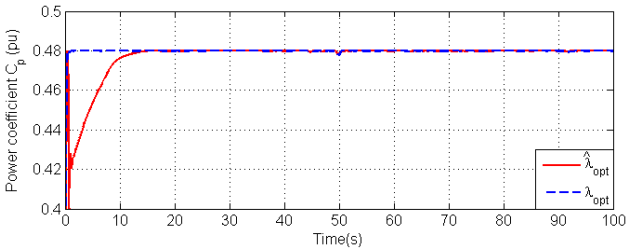

(d)

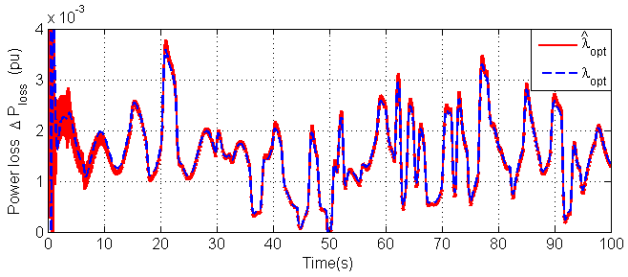

(e)

Figure 6. Simulation results for the embedded ES: (a) error in rotor speed, and (b) error in d-axis current, (c) tip-speed ratio, (d) power coefficient, (e) Power loss in the stator winding.

CONCLUSION

In this paper, a new application of the ES algorithm is proposed. Along with that, a new control law for the machine side converter of the PMSG wind turbine is also designed for both active current and rotor speed adjustment to minimize the power loss in the stator winding and to maximize the absorbed power of the wind turbine system.

The controller is based on a cascade PI controller, accompanying with the Linear Quadratic Regulator (LQR) to optimize the efficiency of this controller. Besides that, the proposed scheme is verified through the simulation results, which is compared to the case of a conventional method. As a result, the proposed control law has obviously a better performance than the conventional PI. And, this performance of the proposed ES application is like the case of exactly-known turbine knowledge which emphasizes the contribution of this paper. The wind turbine can ensure to track the maximum power point tracking curve, whereas the power loss in the generator is the minimum.

ACKNOWLEDGEMENTS

This work was supported by The University of Danang, University of Science and Technology, code number of Project: T2018-02-02.

REFERENCES

[1] Abdullah M., Yatim A.H.M. Tan C.W. and Saidur R.., 2012, "A review of maximum power point tracking algorithms for wind energy systems," Renew. Sustain. Energy Rev., 16 (5), pp. 3220-3227.

[2] Fernando J. L., Godpromesse K., Francoise L. L., 2016, "A novel online training neural network-based algorithm for wind speed estimation and adaptive control of PMSG wind turbine system for maximum power extraction," Renew. Energy, 86, pp. 38-48.

[3] Pucci M. and Cirrincione M., 2011, "Neural MPPT control of wind generators with induction machines without speed sensors," IEEE Trans. Ind. Electron., 58(1) pp. 37-47.

[4] Azad G., Miroslav K., Sridhar S., 2014, "Power optimization and control in wind energy conversion systems using extremum seeking," IEEE Trans. Control Syst. Technol., 22(5), pp. 1684-1695.

[5] Wang C. N., Lin W. C., and Le X. K., 2014, "Modelling of a PMSG wind turbine with autonomous control," Math. Probl. Eng., 2014, pp. 1-9.

[6] Cheng X., Aït-Ahmed M., Benkhoris M. F., Aït-Ramdane N. and Tang T., 2016, "Robustness improvement by using Linear Quadratic Regulator control for PMSG," IEEE Annu. South. Power Electron. Con. (SPEC).

[7] Subashini N., Dharmalingam V. and Uma G., 2015, "Design and implementation of a linear quadratic regulator controlled active power conditioner for effective source utilisation and voltage regulation in low-power wind energy conversion systems," IET Power Electron., 8(11), pp. 2145-2155.

[8] Kartik B. A. and Miroslav K., 2004, "Real-Time optimization by extremum-seeking control," John Wiley & Sons, Inc., Hoboken, New Jersey.

[9] Murray R. M., "Lecture 2 LQR control, control and dynamical systems," Calif. Inst. Technol., Asses 10.11.2017 from World Wide Web: https://www.cds.caltech.edu/murray/courses/cds110/wi06/lqr.pdf.

[10] Hua Y., Bo Y., Li X. and Kai S., 2017, "Modeling and simulation of multi-scale transients for PMSG-based wind power systems," Wind Energy, 20, pp. 1349-1364.

[11] Wu B., Lang Y., Zargari N., Kouro S., 2011, "Power conversion and control of wind energy systems," Willey&Sons, Inc, Koboken, New Jersey.